

Journal Pre-proofs

Platinum(IV) complexes conjugated with chalcone analogs as dual targeting anticancer agents: *in vitro* and *in vivo* studies

Xiaochao Huang, Zhikun Liu, Meng Wang, Xiulian Yin, Yanming Wang, Lumei Dai, Hengshan Wang

PII: S0045-2068(20)31728-4
DOI: <https://doi.org/10.1016/j.bioorg.2020.104430>
Reference: YBIOO 104430

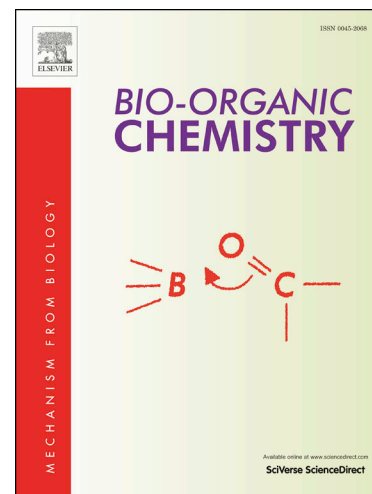
To appear in: *Bioorganic Chemistry*

Received Date: 15 May 2020
Revised Date: 22 September 2020
Accepted Date: 23 October 2020

Please cite this article as: X. Huang, Z. Liu, M. Wang, X. Yin, Y. Wang, L. Dai, H. Wang, Platinum(IV) complexes conjugated with chalcone analogs as dual targeting anticancer agents: *in vitro* and *in vivo* studies, *Bioorganic Chemistry* (2020), doi: <https://doi.org/10.1016/j.bioorg.2020.104430>

This is a PDF file of an article that has undergone enhancements after acceptance, such as the addition of a cover page and metadata, and formatting for readability, but it is not yet the definitive version of record. This version will undergo additional copyediting, typesetting and review before it is published in its final form, but we are providing this version to give early visibility of the article. Please note that, during the production process, errors may be discovered which could affect the content, and all legal disclaimers that apply to the journal pertain.

© 2020 Elsevier Inc. All rights reserved.



Platinum(IV) complexes conjugated with chalcone analogs as dual targeting anticancer agents: *in vitro* and *in vivo* studies

Xiaochao Huang^{a, b 1}, Zhikun Liu^{c 1}, Meng Wang^{a *}, Xiulian Yin^a, Yanming Wang^a, Lumei Dai^d
* and Hengshan Wang^{b *}

^a Jiangsu Key Laboratory of Regional Resource Exploitation and Medicinal Research, and National & Local Joint Engineering Research Center for Mineral Salt Deep Utilization, Huaiyin Institute of Technology, Huaian 223003, China.

^b State Key Laboratory for the Chemistry and Molecular Engineering of Medicinal Resources, School of Chemistry and Pharmaceutical Sciences of Guangxi Normal University, Guilin 541004, China.

^c Jiangsu Province Hi-Tech Key Laboratory for Biomedical Research, Southeast University, Nanjing 211189, China.

^d Key Laboratory of Tropical Marine Bio-resources and Ecology, South China Sea Institute of Oceanology, Chinese Academy of Sciences, Guangzhou 510301, China.

Abstract: For the sake to develop novel platinum(IV) complexes to reverse cisplatin (CDDP) resistance, four multifunctional platinum(IV) prodrugs via conjugating chalcones with the related platinum(IV) complexes derived from cisplatin were designed and evaluated for anti-tumor activities *in vitro* and *in vivo*. Among them, complex **9** exhibited excellent anticancer activities *in vitro* with IC₅₀ values at the submicromolar level against the tested human cancer cells, whereas showed low cytotoxicity towards human normal liver cells HL-7702. Further mechanistic studies indicated that complex **9** induced G2/M phase arrest and apoptosis in A549 cells, which was associated with a collapse of the mitochondrial membrane potential (MMP), alterations in the expression of some apoptosis-related proteins, and enhanced level of the intracellular reactive oxygen species (ROS). More importantly, complex **9** significantly suppressed the tumor growth in the A549 xenograft model without obvious hints of toxicity.

Key words: Platinum(IV) complexes; anti-tumor activity; tubulin; chalcones; apoptosis

* Corresponding author.

E-mail addresses: vipmengwang@126.com; dlmei610@163.com; whengshan@163.com.

¹ Co-first author: These authors contributed equally to this work.

1. Introduction

The uncontrolled and rapid proliferation property of cancer and the high cost of its treatment were main cause encouraging the development for novel and effective chemotherapeutic agents as well as low cytotoxicity to normal cells [1]. Among chemotherapeutic agent targets, tubulin polymerization is an attractive choice owing to the microtubule system plays an important role in essential cellular processes, such as intracellular transport, cell signaling and cell shape organization, respectively [2-4]. Up to now, sever microtubule targeting agents including paclitaxel, docetaxel, and vinblastine have been successfully used chemotherapeutically against various human solid tumors and additional candidates such as combretastatin-A4 (CA-4) and its derivatives were also in clinical trials [5-9]. Moreover, it has been found that chalcone-derived compound **1a** (**Fig. 1**) exhibits strongly inhibition on the growth of cancer cell lines including multi-drug resistance cells and tubulin polymerization by binding to the colchicine site of tubulin [10, 11]. However, the utilization of microtubule targeting agents in clinic has been hampered by drug resistance, low bioavailability and serious side effects [12-14].

Platinum(II) complexes (**Fig. 2**), such as cisplatin, carboplatin and oxaliplatin, which usually considered as a class of alkylating agents, are indispensable choices for various solid tumors in clinic due to its high efficiency [15-17]. Until now, CDDP, which mainly interacts with DNA, induces the blockage of replication and transcription and ultimately causes death of tumor cells, have been widely used in the clinical treatment of different solid tumors [18, 19]. However, all these platinum(II)-based agents are associated with multi-drug resistance and severe side effects including nephrotoxicity, myelosuppression, and neurotoxicity during the clinical chemotherapy [20-22], which has further driving the search for new and effective platinum complexes with satisfactory antitumor activities and low toxicity to normal cells.

In recent years, the potential therapeutic effects of platinum(IV) complexes for cancer treatment have attracted broad attention [23]. Notably, platinum(IV) complexes possess several advantages compared to their platinum(II) complexes, such as their better toxicological profile and possibility of oral administration as well as acting as prodrugs of their platinum(II) counterparts, respectively [23, 24]. More importantly, platinum(IV) complexes cloud offer two valuable axial positions in comparison to their platinum(II) counterparts, which afford a higher molecular diversity and more potential for drug optimization, resulting in various hybrid compounds (e.g., multi-target

compounds) [25, 26]. Until now, such platinum(IV) hybrid compounds (**Fig. 2**) as Asplatin, Mitaplatin, NERi-Pt(IV) and Cx-platin exhibited remarkable anticancer activities against human cancer cells including cisplatin-resistant cell lines owing to the introduction of the bioactive moiety to the axial position [27-30]. Thus, it can be imagined that the combination of platinum(IV) complexes derived from cisplatin with tubulin inhibitor **1a** could remarkably improve therapeutic profiles and overcome the side effect as well as multi-drug resistance of cisplatin.

Previously, we reported a dual-targeting platinum(IV) prodrugs derived from CA-4, proving that microtubule inhibitor-derived platinum(IV) complexes enhanced anti-tumor activities *in vitro* and reverse cisplatin resistance in lung cancer [30b]. Taken the advantages of both microtubule inhibitor and platinum complexes in consideration, four dual-targeting platinum(IV) prodrugs, which made structural modifications to **1a** by introducing platinum(IV) complexes derived from cisplatin, were synthesized and prepared as shown in **Scheme 1**. These platinum(IV) complexes were characterized and evaluated for antitumor activities *in vitro* and *in vivo*, and their underlying cytotoxic mechanisms were also investigated.

2. Results and discussion

2.1. Synthesis and characterization.

As shown in **scheme 1**, compound **1a** was obtained by Claisen-Schmidt condensation of **1** and **2** in the presence of KOH (50% w/v aqueous solution) in methanol at 0 °C for overnight. Then esterification reaction of compound **1a** with succinic anhydride or glutaric anhydride in the presence of potassium carbonate in N,N-Dimethylformamide (DMF) gave compound **4** and **5**. In addition, the synthesis of two platinum(IV) complexes **5** and **6** were prepared through the oxidative reaction of the cisplatin with H₂O₂ or N-chlorosuccinimide (NCS) in water according to the reported procedure [31]. Finally, the target platinum(IV) complexes **7-10** were obtained by esterification between **3** or **4** and **5** or **6** in the presence of O-(benzotriazol-1-yl)-N,N,N',N'-tetramethyluronium tetrafluoroborate (TBTU) and Et₃N in DMF. Meanwhile, the resulting title target platinum(IV) complexes **7-10** were characterized by ¹H NMR, ¹³C NMR, ¹⁹⁵Pt spectra and elemental analysis together with ESI-MS spectroscopy.

2.2. In vitro cytotoxicity.

In present work, the cytotoxicity of the synthesized target platinum(IV) complexes **7-10** were evaluated their anti-proliferative activities against HeLa (cervical), MGC-803 (gastric), HepG-2

(hepatocellular), NCI-H460 (non-small-cell lung carcinoma) and human normal liver cells HL-7702 using MTT (3-(4,5-dimethylthiazol-2-yl)-2,5-diphenyltetrazolium bromide) assay, using compound **1a** and cisplatin as positive drugs. As shown in Table 1, the positive drug **1a** exhibited excellent anticancer activities against the tested human cancer cells, with IC_{50} values at submicromolar level as expected, which urged us to search for potential compounds with better activities. We then evaluated the anti-proliferative activity of platinum(IV) complexes **7-10**, for which were attached to an inhibitor of tubulin **1a** at one axial position of platinum(IV) complexes octahedral coordination sphere via a linker. Similarly, compounds **3** and **4** were performed as controls. The results listed in Table 1 indicated that these platinum(IV) complexes **7-10** displayed excellent antitumor activities toward tested human cancer cell lines, possessed higher antitumor activity and lower cytotoxicity than that of **1a** and cisplatin. Among them, complex **9** exhibited very good activity with IC_{50} values that ranged from 0.26 to 0.37 μ M against the four human cancer cell lines, which exhibited a 21.2~29.4 fold increase in activity than that of cisplatin, respectively. Notably, complexes **9** (IC_{50} value of 12.35 μ M) also exhibited lower cytotoxicity against human normal liver cells HL-7702 than that of cisplatin (IC_{50} value of 10.36 μ M) and **1a** (IC_{50} value of 3.07 μ M), and the selectivity index (SI) of complex **9** (SI of 42.6) synchronously exhibited much higher than that of the positive drugs cisplatin (SI of 1.3) and **1a** (SI of 7.3), respectively. Not surprisingly, compounds **3** and **4**, derivatives of compound **1a**, inherited efficient antitumor activity with IC_{50} values ranged from 0.52 to 1.35 μ M against cancer cells tested in this work, while showed high SI to HL-7702 (SI values of 11.4 and 14.8, respectively). More importantly, complexes **7** and **9** exhibited better antitumor activities compared to complexes **8** and **10**, indicating that the axial ligand from hydroxyl group to chloride can obviously result in different activity, respectively.

2.3. Anti-proliferative activity of complex **9** against drug-resistant cancer cells.

Previous studies indicated that development of multidrug resistance to first-line chemotherapy drugs, such as cisplatin and doxorubicin (DOX), was an importantly reason for the failure of most first round chemotherapy [20, 32]. Accordingly, it will be interesting to further evaluate if our synthesized target compounds, which were platinum(IV) complexes derived from cisplatin, could also overcome the multidrug resistance. Therefore, the most active complex **9** was selected to test the cytotoxicity against cisplatin-resistant cells (A549/CDDP) together with doxorubicin-resistant cells (MCF-7/DOX), using compound **1a**, cisplatin and compound **4** as controls. As shown in Table

2, cisplatin exerted poor anti-proliferation activity against A59/CDDP cells (IC_{50} value of 35.06 μ M and resistant factor (RF) of 5.5, respectively), while DOX against MCF-7/CDDP cells (IC_{50} value of 42.71 ± 2.01 μ M and RF of 14.1, respectively) was also obviously decreased compared with sensitive cancer cell lines. Interestingly, it was noted that complex **9** could remarkably inhibit the proliferation of the cell lines A549/CDDP (IC_{50} value of 0.23 μ M and RF of 1.2, respectively) and MCF-7/DOX (IC_{50} value of 0.42 μ M and RF of 1.1, respectively) with very small resistant factor values. Similarly, compound **4** showed great potential anti-tumor activity against A549 and A549/CDDP cells (IC_{50} values were 0.65 ± 0.13 μ M and 0.83 ± 0.11 μ M), and exhibited moderate anti-proliferation activity against MCF-7 and MCF-7/DOX cells (IC_{50} values were 1.76 ± 0.27 μ M and 2.33 ± 0.39 μ M), respectively. Moreover, the combined group (compound **4** and CDDP) seemed to reverse cisplatin resistance in A549/CDDP cells with RF value of 2.0, which was higher than that of complex **9** but lower than cisplatin. In shorts, these results indicated that complex **9** exhibited potent anti-MDR potential and deserved further study, which might be useful in the treatment of drug refractory cancer resistance to cisplatin.

2.4. Antitumor effect of complex **9** *in vivo*.

Compound **9** was chosen to evaluate the *in vivo* antitumor efficacy owing to its excellent anticancer activity against the tested human cancer cells including multidrug-resistant cells. Thus, to further evaluate the antitumor potency of complex **9** *in vivo*, we established xenograft models by subcutaneously injecting A549 cells at the logarithmic growth phase into the right armpit of mice. When the model was well-established, mice with tumors at the volume of 100-150 mm³ were randomly divided into four groups (n=5/group): (1) vehicle treated group (5% dextrose injection), (2) cisplatin (5 mg/kg) treated group, (3) compound **1a** (5 mg/kg) treated group, (4) compound **9** (5 mg/kg) treated group, (5) compound **9** (13 mg/kg) treated group, respectively. We collected and weighed the tumors and calculated the inhibition rate of tumor growth (IRT) at the end of treatment. As exhibited in **Fig. 3 B and D**, the growth of A549 tumor xenograft was effectively suppressed by 58.7% and 68.7% (IRT) after treatment groups were injected with compound **9** at two doses (5 and 13 (mg/kg)/7days) for three weeks in the A549 tumor model, respectively. Notably, compound **9** displayed better *in vivo* antitumor activity than those of **1a** (IRT, 62.5%) and cisplatin (IRT, 65.7%) after administration of compound **9** at high dosage (13mg/kg), respectively. More importantly, compound **9** displayed lower toxicity compared to the positive drugs cisplatin and **1a** *in vivo*, as

evidenced by changes in the weight of the mice after iv administration at 13 mg/kg of compound **9** in the entire observation period (**Fig. 3 C**).

2.5. Anticancer mechanism of complex **9**.

2.5.1 The release of compound **4** under the reduction of vitamin C.

Based on the concept of prodrugs, platinum(IV) complexes could release compound **4** and corresponding platinum(II) complexes under reducing condition (such as vitamin C) [23, 24]. Therefore, complex **9** was chosen for *in vitro* release assays via reversed phase high performance liquid chromatography (RP-HPLC), using vitamin C (2.211 min), compound **4** (12.785 min) as controls to match the peaks during the release process of complex **9**. Firstly, we investigated the stability of complex **9** in physiological environment (PBS, pH = 7.4), and the merged chromatograms in **Fig. S1E** showed that complex **9** was stable and was not decomposed in 72 h. However, when co-incubated with vitamin C (3.0 equiv.), the peak at 9.101 min of complex **9** gradually decreased along with another increasing peak (12.785 min), which appeared right at the position of compound **4**, indicating that complex **9** successfully decomposed compound **4** and cisplatin. Not surprisingly, the cisplatin was not be detected under this condition of liquid conditions due to its weak UV absorption, which had been reported previously [11,18, 20, 24]. To investigate whether complex **9** can be reduced to compound **4** in equivalents, standard curve of compound **4** was established. As illustrated in **Fig. S1H**, after 3 h co-incubation of vitamin C, 1.8 μ M of complex **9** can release almost the same concentration of compound **4** (1.78 μ M), indicating that the target complex **9** could be acted as platinum(II) prodrug. Furthermore, 4.5 h co-treatment with carboxylesterase only led ~60 % of complex **9** decomposition to compound **1a**, whereas ~100 % of complex **9** was deducted within 3 h under reduction of vitamin C, showing that the anticancer activities induced by complex **9** was mainly contributed to the strategy of platinum(IV) prodrug rather esterase.

2.5.2 Analysis of immunofluorescence staining.

Many studies indicated that tubulin was an essential eukaryotic protein that plays an important role in cell division and basic cellular functions [6, 7]. In order to investigate whether the activity of complex **9** was related to the interaction with microtubule systems, here, we determined the effect of optimal compounds on the microtubule cytoskeleton of A549 cells using immunofluorescence assay. As exhibited in **Fig.4**, in the control groups, the microtubule network in the A549 cells

showed normal arrangement and organization, characterized by regularly assembled in the absence of drug treatment. After treatment with compound **1a** at a concentration of 10 μM , cells displayed obviously disrupted microtubule organization as expected (**Fig.4**). Interestingly, cells after exposure to complex **9** at 5 and 10 μM for 24 h, the spindle microtubule organization was significantly deranged, and the nucleus of the cells narrowed sharply and the spindle microtubules were heavily disrupted microtubule organization, respectively (**Fig.4**).

2.5.3 Complex 9 induced apoptosis in A549 cells.

In order to investigate the capacity of complex **9** to induce apoptosis in human lung cancer cells A549, thus, a FITC conjugated annexin-V/PI assay was performed with A549 cells. As shown in **Fig.5**, after A549 cells were exposed to 10 μM of the cisplatin for 24 h, the total fractions of early apoptotic cells (Q4) and late apoptotic cells (Q2) was 11.93% compared with 2.74%. Notably, after A549 cells were exposed to 5.0 or 10 μM of the complex **9** for 24 h, the total fractions of early apoptotic cells (Q4) and late apoptotic cells (Q2) were 14.8% and 23.06%, respectively.

2.5.4 Cell uptake.

Since compound **9** exhibited the most potent antitumor activity in the cellular assays, according to the former reported, which may be partly attributed to the increased cellular uptake [20]. In order to this hypothesis, here, we selected inductively coupled plasma-mass spectrometry (ICP-MS) to carry out the intracellular platinum content in A549 cells. Notably, as exhibited in Table 3, after A549 cells exposure to 10 μM of compound **9** for 12 h, the concentration of cellular platinum increase to 263 ng/ 10^6 cells, which was nearly up to 2.24-fold as much as that of cisplatin (263 ng/ 10^6 cells). In brief, the outcomes of this experimental seem to exhibit that the improvement of cellular uptake could result in enhanced therapeutic profiles.

2.5.5 Cell cycle analysis.

To gain deeper insight on the mode of action, the most valid compound **9** was examined for its effect on cell cycle progression of A549 cells by flow cytometry. As shown in **Fig. 6**, incubation of compound **9** at the indicated concentrations for 24 h led to a gradual accumulation of A549 cells in the G2/M phase of the cell cycle in a dose-dependent manner, but the control group cells were primarily in the G1 and S stage. Notably, the cell cycle was obviously changed after treatment with compound **9** at 5.0 and 10 μM for 24 h: the percentage of G2/M phase increases to 72.79% and 86.42% compared to the control group cells, with a concomitant decrease of cells in the G1 and S

phase cells. Moreover, the percentage of A549 cells in the G2/M and S phase increased to 16.09% and 54.21%, respectively, after incubation with cisplatin at 10 μ M for 24 h (**Fig. 6**). Thus, these results indicated that compound **9** caused arrest in the G2/M phase in human lung cancer cells A549.

2.5.6 Complex 9 inhibited the migration of A549 cells in vitro

Increasing evidence indicated that cancer cell migration was one of the important causes resulting to the death of tumor patients [33]. Thus, in order to further investigate the inhibitory ability of complex **9** to cell motility, a well-established wound-healing assay was conducted to investigate whether complex **9** could inhibit the migration of A549 cells. As exhibited in **Fig. 7**, in comparison to the control group, the wound closure of the migration was remarkably suppressed for complex **9** treated groups. Notably, the inhibition rate of migration was in the order of complex **9** treated groups > cisplatin treated groups > control groups. In shorts, these results suggested that complex **9** showed a significant inhibitory effect on migration of human lung cancer cells A549, and may be a promising candidate lead compound for chemotherapy of metastatic cancer.

2.5.7 Complex 9 triggered mitochondrial pathway dependent apoptosis.

Many studies indicated that decreased MMP has been implicated as an important event in apoptotic cells [34-36]. To further investigate the contribution of mitochondria in complex **9** induced cell apoptosis, here we utilized a quantitative MMP assay to measure the activities of JC-1 stained mitochondria and detected by flow cytometry analysis in A549 cells. As presented in **Fig. 8**, the MMP level in A549 cells was decreased to 88.20% compared to control group cells (97.41%) after treatment with cisplatin at 10 μ M for 24 h. In comparison of control cells, it was noted that the MMP level in A549 cells was decreased from 84.83% to 72.77%, respectively, after incubation of complex **9** at 5.0 and 10 μ M for 24 h (**Fig. 8**), suggesting that complex **9** decreased the MMP of A549 cells during the apoptosis process.

2.5.8 Complex 9 triggered reactive oxygen species (ROS) generation.

According to previous reported, compromised mitochondria could significantly induce an increase in ROS levels [37, 38], which can in turn lead to cell apoptosis [39, 40]. In order to further investigate the deeper mechanism of complex **9** for inhibiting tumor cells, therefore, we evaluated the ability of complex **9** to induce ROS in human lung cancer cells A549 using 2', 7'-dichlorofluoresceindiacetate (DCFH-DA) fluorescent probe. As the results illustrated in **Fig. 9**, the generation of ROS level was enhanced to 14.81% compared to the control cells (2.32%) after

treatment with cisplatin at 10 μ M for 24 h. Moreover, complex **9** induced the generation of ROS level in a concentration-dependent manner, and the generation of ROS level in human lung cancer cells A549 was increased from 27.93% to 46.57%, respectively. More importantly, as presented in **Fig. 9**, it was worth noted that the generation of ROS level was nearly up to 3.14-fold as much as that of cisplatin after cells exposure to 10 μ M of complex **9** for 24 h, respectively. In shorts, these results seem to indicate that ROS may mediate A549 cells apoptosis in the presence of complex **9**.

2.5.9. Complex 9 induced apoptosis via the activation of caspases and regulated apoptosis-related protein expression.

Increasing evidence has indicated that the regulation of the Bcl-2 family of proteins was involved in the signaling pathways [41]. Accordingly, several apoptotic-related proteins such as Bcl-2 (anti-apoptotic protein) and Bax (pro-apoptotic protein) were investigated using western blot assay. As the results illustrated in **Fig. 10**, in comparison of control cells, A549 cells after incubation of complex **9** at the indicated concentrations (2.5, 5.0 and 10 μ M), the level of anti-apoptotic protein Bcl-2 was efficiently down-regulated, whereas the pro-apoptotic protein Bax was up-regulated significantly. Moreover, according to previous reported, the caspases protein family including caspase-3 and caspase-9, were known as an important executioner caspases in cell apoptosis [42]. Therefore, we further investigated whether the caspase-3 and -9 was activated by complex **9** using western blot assay. As presented in **Fig.10**, complex **9** remarkably up-regulated the expression level of caspase-3 and -9 at the indicated concentrations, whereas cisplatin had little influence on them.

3. Conclusions

Many strategies have been developed to overcome the shortcomings of cisplatin, however the inherent problems were still not resolved well. In the present study, here four tubulin-targeting platinum(IV) prodrugs were successfully synthesized and evaluated for anti-proliferative activity using MTT assay. The results of MTT activity test *in vitro* indicated that these four platinum(IV) complexes **7-10** not only showed greater potency in anti-proliferative activity compared to the positive drugs cisplatin and **1a** against tested human cancer cells including multidrug-resistant cancer cell lines, but also exhibited lower cytotoxicity than that of positive drugs (cisplatin and **1a**) toward human normal liver HL-7702, respectively. Especially, complex **9** displayed the most potent anti-proliferative activities against tested human cancer cell lines with IC₅₀ values of 0.19~0.37 μ M. Moreover, complex **9** significantly induced cell apoptosis, caused cell cycle arrest at G2/M phase

and obviously disrupted the microtubule organization, respectively. Cellular studies revealed that the induction of apoptosis by complex **9** was associated with a collapse of the MMP, and enhancing the intracellular ROS level, and alterations in the expression of apoptosis related proteins (e.g., Bax and Bcl-2, respectively). In addition to these mechanism studies, we further investigated the antitumor potency of complex **9** *in vivo*. *In vivo* experiment results revealed that complex **9** could significantly inhibit tumor growth in the A549 xenograft model, and had no observable toxic effect during the test. Taken together, these *in vitro* and *in vivo* results indicated that complex **9** may be promising lead compounds for the development of new anticancer drugs.

4. Experimental section

All chemicals and solvents were analytical reagent grade and commercially available, and the column chromatography was performed using silica gel (200–400 mesh). ¹H NMR and ¹³C NMR spectra were recorded in CDCl₃ or DMSO-*d*₆ with a Bruker 400 or 600 MHz NMR spectrometer, and the mass spectra were measured on an Agilent 6224 TOF LC/MS instrument. In addition, the elemental analyses of C, H, and N used a Vario MICRO CHNOS elemental analyzer (Elementary)

4.1. General procedure for the preparation of compounds.

4.1.1. (*E*)-3-(3-hydroxy-4-methoxyphenyl)-1-(3,4,5-trimethoxyphenyl)prop-2-en-1-one (**1a**)

To a solution of compound **1** (2.1 g, 10.0 mmol) and **2** (1.52 g, 10.0 mmol) in methanol (20 mL) was cooled to ice-water, and the 50% KOH (10 mL, aq) added to dropwise to the reaction, and then the mixture stirred at ice-water for overnight. After completion of reaction, the mixture was poured into ice-water (200 mL), and adjusted to pH = 1~2 with 4 N HCl. The precipitated was filtered, washed with water and dried to offer the crude product which was purified by chromatography on silica gel to obtain **1a** as a yellow solid (yield: 2.6 g, 75.6%). ¹H NMR (600 MHz, CDCl₃) δ 7.73 (d, *J* = 15.5 Hz, 1H), 7.34 (d, *J* = 15.5 Hz, 1H), 7.29 (d, *J* = 2.1 Hz, 1H), 7.26 (s, 2H), 7.13 – 7.11 (m, 1H), 6.86 (d, *J* = 8.3 Hz, 1H), 5.81 (s, 1H), 3.94 (s, 6H), 3.93 (s, 3H), 3.92 (s, 3H). ¹H NMR (600 MHz, CDCl₃) δ 7.74 (d, *J* = 15.5 Hz, 1H), 7.35 (d, *J* = 15.5 Hz, 1H), 7.30 (d, *J* = 2.1 Hz, 1H), 7.27 (m, 2H), 7.13 – 7.11 (m, 1H), 6.87 (d, *J* = 8.3 Hz, 1H), 5.82 (s, 1H), 3.94 (s, 6H), 3.93 (s, 3H), 3.93 (s, 3H). HR-MS (*m/z*) (ESI): calcd for C₁₉H₂₀O₆ [M-H]⁻: 343.1182; found: 343.1060.

4.1.2. General procedure for preparing compounds **3-4**.

Synthesis of compounds **3** and **4**. To a solution of **1a** (2.5 g, 7.3 mmol) and anhydrous K₂CO₃ (2.0 g, 14.6 mmol) in DMF (15 mL), succinic anhydride (35.6 mmol) or glutaric anhydride (35.6

mmol) was added, and the mixture reaction was stirred at 50 °C for 1 h and monitored by TLC. After completion of reaction, the mixture was adjusted to pH = 2~3 with 2 N HCl, and then the mixture was added dichloromethane (150 mL), washed with water (3×300 mL), and the combined organic phase was dried over anhydrous Na₂SO₄ and concentrated under reduced pressure. The residue was purified on silica gel column eluted methanol/dichloromethane to obtain the desired compound **3** or **4**.

(*E*)-4-(2-methoxy-5-(3-oxo-3-(3,4,5-trimethoxyphenyl)prop-1-en-1-yl)phenoxy)-4-oxobutanoic acid (**3**). 2.2 g, 67.9% yield as a yellow solid. ¹H NMR (600 MHz, DMSO-*d*₆) δ 9.15 (s, 1H), 7.71 (d, *J* = 15.4 Hz, 1H), 7.63 (d, *J* = 15.4 Hz, 1H), 7.40 (s, 2H), 7.38 (d, *J* = 2.1 Hz, 1H), 7.31 – 7.29 (m, 1H), 7.00 (d, *J* = 8.4 Hz, 1H), 3.90 (s, 6H), 3.84 (s, 3H), 3.76 (s, 3H), 2.92 – 2.87 (m, 4H). HR-MS (*m/z*) (ESI): calcd for C₂₃H₂₄O₉ [M+Cl]⁻: 479.1109; found: 479.0947.

(*E*)-5-(2-methoxy-5-(3-oxo-3-(3,4,5-trimethoxyphenyl)prop-1-en-1-yl)phenoxy)-5-oxopentanoic acid (**4**). 2.4 g, 72.7% yield as a yellow solid. ¹H NMR (600 MHz, DMSO-*d*₆) δ 12.19 (s, 1H), 7.84 (d, *J* = 15.5 Hz, 1H), 7.82 (d, *J* = 2.1 Hz, 1H), 7.75 – 7.73 (m, 1H), 7.71 (d, *J* = 15.4 Hz, 1H), 7.43 (s, 2H), 7.21 (d, *J* = 8.6 Hz, 1H), 3.90 (s, 6H), 3.84 (s, 3H), 3.76 (s, 3H), 2.65 (t, *J* = 7.4 Hz, 2H), 2.39 (t, *J* = 7.3 Hz, 2H), 1.90 – 1.85 (m, 2H). HR-MS (*m/z*) (ESI): calcd for C₂₄H₂₆O₉ [M+Cl]⁻: 493.1265; found: 493.1075.

4.1.3. General procedure for preparing compounds **5**, **6**.

H₂O₂ (30 wt%, 33.3 mmol) or N-chlorosuccinimide (NCS) (534.1 mg, 4.0 mmol) in 10 mL water was added dropwise to a solution of cisplatin (1.0 g, 3.33 mmol) in water (30 mL) at temperature. After that, the reaction solution was heated to 50 °C for 10 h. Process of the reaction was monitored with TLC and visualized with iodine in silica gel. Part of the solution was removed under reduced pressure, after completion of the reaction. The yellow crystal solid obtained was filtered, washed with water, cold ethanol and ether. Final target product was dried at dark in vacuum to give yellow solid.

cis,cis,trans-[Pt(NH₃)₂Cl₂(OH)₂] (**5**). Yellow solid (812 mg). Yield 72.5 %. IR (KBr): 3512 (s, OH stretch), 1036 (s, Pt-OH bend), 549 (m, Pt-N(O) stretch). Elemental Analysis (%): H, 2.41; N, 8.39; found H, 2.43; N, 8.47.

cis,cis,trans-[Pt(NH₃)₂Cl₂((OH)(Cl))] (**6**). Yellow solid (600 mg). Yield 51.2 %. ¹H NMR (600 MHz, DMSO-*d*₆) δ 5.76 – 5.50 (m, 6H), 1.50 (s, 1H).

4.1.4. General procedure for preparing compounds **7-10**.

To a solution of **3** (150 mg, 0.327 mmol) or **4** (150 mg, 0.33 mmol), TBTU (158 mg, 0.491 mmol), and Et₃N (50 mg, 0.491 mmol) in dry DMF (3 mL), complex **5** or **6** (0.327 mmol) was added in reaction. The reaction was stirred at 30 °C for overnight and monitored by TLC. The mixture reaction was added to CH₂Cl₂ (150 mL), and then extracted twice with water (150 mL), and the organic layer was dried over anhydrous Na₂SO₄ and concentrated under reduced pressure. The residue was purified on silica gel column eluted methanol/dichloromethane to obtain the desired product **7**, **8**, **9** or **10**.

cis,cis,trans-[Pt(NH₃)₂Cl₂((E)-2-methoxy-5-(3-oxo-3-(3,4,5-trimethoxyphenyl)prop-1-en-1-yl)phenyl succinate (OH)] (**7**). 100 mg, 40.5% yield as a yellow solid. ¹H NMR (600 MHz, DMSO-*d*₆) δ 7.84 – 7.81 (m, 2H), 7.75 – 7.73 (m, 1H), 7.71 (d, *J* = 15.4 Hz, 1H), 7.42 (s, 2H), 7.20 (d, *J* = 8.6 Hz, 1H), 6.06 – 5.81 (m, 6H), 3.90 (s, 6H), 3.84 (s, 3H), 3.76 (s, 3H), 2.76 (t, *J* = 7.1 Hz, 2H), 2.57 (t, *J* = 7.1 Hz, 2H). ¹³C NMR (150 MHz, DMSO-*d*₆) δ 188.15, 179.42, 171.18, 153.42, 153.38, 143.65, 142.38, 140.13, 133.58, 129.86, 128.12, 122.99, 120.68, 113.27, 106.63, 60.67, 56.82, 56.62, 31.64, 30.37. ¹⁹⁵Pt NMR (129 MHz, DMSO-*d*₆): δ/ppm 1229.10; HR-MS (*m/z*) (ESI): calcd for C₂₃H₃₀Cl₂N₂O₁₀Pt [M+Cl]⁺:794.0614; found: 795.0308. Elemental analysis calcd (%) for C₂₃H₃₀Cl₂N₂O₁₀Pt: C, 36.33; H, 3.98; N, 3.68; found: C, 36.46; H, 4.03; N, 3.39.

cis,cis,trans-[Pt(NH₃)₂Cl₂((E)-2-methoxy-5-(3-oxo-3-(3,4,5-trimethoxyphenyl)prop-1-en-1-yl)phenyl succinate)(Cl)] (**8**). 125 mg, 49.2% yield as a yellow solid. ¹H NMR (600 MHz, DMSO-*d*₆) δ 7.84 – 7.81 (m, 2H), 7.75 – 7.73 (m, 1H), 7.70 (d, *J* = 15.4 Hz, 1H), 7.42 (s, 2H), 7.20 (d, *J* = 8.6 Hz, 1H), 6.10 – 5.80 (m, 6H), 3.90 (s, 6H), 3.84 (s, 3H), 3.76 (s, 3H), 2.76 (t, *J* = 7.1 Hz, 2H), 2.57 (t, *J* = 7.2 Hz, 2H). ¹³C NMR (150 MHz, DMSO-*d*₆) δ 188.17, 179.44, 171.18, 153.42, 153.39, 143.64, 142.41, 140.15, 133.59, 129.84, 128.13, 123.00, 120.71, 113.29, 106.67, 60.67, 56.83, 56.63, 31.67, 30.38. ¹⁹⁵Pt NMR (129 MHz, DMSO-*d*₆): δ/ppm 548.03; HR-MS (*m/z*) (ESI): calcd for C₂₃H₂₉Cl₃N₂O₉Pt [M+H]⁺:778.0665; found: 778.0673. Elemental analysis calcd (%) for C₂₃H₂₉Cl₃N₂O₉Pt: C, 35.47; H, 3.75; N, 3.60; found: C, 35.68; H, 3.61; N, 3.39.

cis,cis,trans-[Pt(NH₃)₂Cl₂((E)-2-methoxy-5-(3-oxo-3-(3,4,5-trimethoxyphenyl)prop-1-en-1-yl)phenyl glutarate)(OH)] (**9**). 105 mg, 41.7% yield as a yellow solid. ¹H NMR (400 MHz, DMSO-*d*₆) δ 7.86 – 7.81 (m, 2H), 7.74 – 7.68 (t, *J* = 11.0 Hz, 2H), 7.42 (s, 2H), 7.20 (d, *J* = 8.5 Hz, 1H), 6.25 – 5.76 (m, 6H), 3.90 (s, 6H), 3.84 (s, 3H), 3.76 (s, 3H), 2.65 (t, *J* = 7.2 Hz, 2H), 2.33 (t, *J* = 7.0

Hz, 2H), 1.87 – 1.81 (m, 2H). ^{13}C NMR (100 MHz, DMSO- d_6) δ 188.15, 180.71, 171.64, 153.38, 143.61, 142.40, 140.19, 133.59, 129.94, 128.20, 122.72, 120.72, 113.28, 106.66, 60.67, 56.76, 56.65, 35.69, 33.15, 21.58. ^{195}Pt NMR (129 MHz, DMSO- d_6): δ /ppm 1228.24; HR-MS (m/z) (ESI): calcd for $\text{C}_{24}\text{H}_{32}\text{Cl}_2\text{N}_2\text{O}_{10}\text{Pt}$ $[\text{M}+\text{H}]^+$:774.1160; found:775.0909. Elemental analysis calcd (%) for $\text{C}_{24}\text{H}_{32}\text{Cl}_2\text{N}_2\text{O}_{10}\text{Pt}$: C, 37.22; H, 4.16; N, 3.62; found: C, 37.46; H, 4.31; N, 3.31.

cis,cis,trans-[Pt(NH₃)₂Cl₂((E)-2-methoxy-5-(3-oxo-3-(3,4,5-trimethoxyphenyl)prop-1-en-1-yl)phenyl glutarate)(Cl)] (10). 123 mg, 47.6% yield as a yellow solid. ^1H NMR (400 MHz, DMSO- d_6) δ 7.86 – 7.81 (m, 2H), 7.74 – 7.68 (m, 2H), 7.42 (s, 2H), 7.20 (d, J = 8.6 Hz, 1H), 6.43 – 6.02 (s, 6H), 3.90 (s, 6H), 3.84 (s, 3H), 3.76 (s, 3H), 2.67 (t, J = 7.4 Hz, 2H), 2.40 (t, J = 7.1 Hz, 2H), 1.89 – 1.82 (m, 2H). ^{13}C NMR (100 MHz, DMSO- d_6) δ 188.15, 180.21, 171.59, 153.38, 143.59, 142.40, 140.18, 133.58, 129.93, 128.21, 122.72, 120.73, 113.29, 106.66, 60.67, 56.76, 56.65, 35.49, 33.04, 21.42. ^{195}Pt NMR (129 MHz, DMSO- d_6): δ /ppm 547.76; HR-MS (m/z) (ESI): calcd for $\text{C}_{24}\text{H}_{31}\text{Cl}_3\text{N}_2\text{O}_9\text{Pt}$ $[\text{M}+\text{Na}]^+$:814.0641; found:815.0348. Elemental analysis calcd (%) for $\text{C}_{24}\text{H}_{31}\text{Cl}_3\text{N}_2\text{O}_9\text{Pt}$: C, 36.35; H, 3.94; N, 3.53; found: C, 36.57; H, 4.01; N, 3.21.

4.2. In vitro cytotoxicity.

All human cancer cell lines (HeLa, NCI-H460, HepG-2, MCF-7, MGC-803, A549, A549/CDDP and MCF-7/DOX) and human normal liver cells (HL-7702) were purchased from the Shanghai Cell Bank of the Chinese Academy of Sciences. Culture medium Roswell Park Memorial Institute (RPMI-1640), phosphate buffered saline (PBS, pH=7.2), fetal bovine serum (FBS), and Antibiotic-Antimycotic came from KeyGen Biotech Company (China). In this study, the cytotoxicity of target compounds was tested using MTT methods. All cancer cell lines were cultivate in the supplemented with 10% FBS, and human normal liver HL-7702 cells were cultivate in the supplemented with 20% FBS, 100 units/ml of penicillin and 100 g/ml of streptomycin in a humidified atmosphere of 5% CO_2 at 37 °C. After that, target compounds and dissolved in DMF (Sigma) and diluted to different concentrations with medium were added to those different cells culture medium, respectively. After 72 h incubation, added to 10 μM of MTT (5 mg/mL) in the cell culture fluid, and the cells were incubated for another 4 h. After 4 h treatment, the medium was replaced with DMSO (100 μL), and the O.D. The value was read with a 570/630 nm enzyme-labeling instrument. All data were independently tested repeated in triplicate.

4.3. The release of compound 4 under the reduction of vitamin C.

In order to investigate the stability of complex **9** in various solutions, RP-HPLC (waters, e2695 system; 2489 UV/Vis detector) assays were carried out. As for the release of compound **4** assays, the stored solutions of complex **9** (2.0 mM, acetonitrile : water= 50 : 50,V/V, 1.0 mL) and vitamin C (60 mM, waster, 100 μ L) were prepared and were incubated at 37 °C in dark. The time-dependent release of compound **4** was monitor with HPLC (UV/Vis, 254 nm). The stability of complex **9** (10.0 mM) in PBS was detected with HPLC (UV/Vis, 254 nm). A solution of complex **9** (1.0 mM, PBS solution with 5% acetonitrile) and carbonate esterase (2.0 unit/mL) was incubated at 37 C in dark and was monitored via HPLC (UV/Vis, 210 nm). Similarly, compound **4**, vitamin C and compound **1a** were recorded as controls. The standard curves of compound **4** (0.025-2.5 mM, acetonitrile) and compound **1a** (0.06-3.0 mM, acetonitrile) were recorded via HPLC and analyzed with graphpad prism 8.0. HPLC conditions: flow rate, 1.0 mL/min; ODS column (250 \times 4.6 mm, 5 μ m), volume of sample injection, 20.0 μ L; column incubator, 35 °C.

4.4. Cell uptake.

The content of cellular uptake of complex **9** was measured on A549 cells, and the cisplatin was served as positive drug. Firstly, A549 cells were seeded in each well of 24-well plates until reached about 80% confluence, and 2.5 and 5.0 μ M of complex **9** and cisplatin were added. The plates were also incubated at an atmosphere of 5% CO₂ and 95% air at 37.0 °C for 12 h. After completion of 12 h incubation, the cells were harvested, washed with ice-cold PBS, centrifuged at 1000 g, and resuspended in PBS (2 mL). The cell numbers were counted by using 100 μ L suspension, and the rest cells were digested with 65% nitric acid at 65 °C for 12 h, and then the Pt level in cells were detected by ICP-MS.

4.5. Cell apoptosis analysis.

A549 cells were grown in each well of six-well plates at the density of 5×10^4 cells/mL of the RPMI-1640 medium with 10% FBS to the final volume of 2 mL. The plates were also incubated at an atmosphere of 5% CO₂ and 95% air at 37.0 °C for overnight, and incubated in the presence or absence of complex **9** and cisplatin at the indicated concentrations for 24 h to induce cell apoptosis. After 24 h treatment, cells were harvested, washed with ice-cold PBS, resuspended in PBS (2 mL) and incubated with 5 μ L of Annexin-V/FITC 5 μ L of PI in the dark at 4 °C for 30 minutes. Finally, the cells analyzed by flow cytometry (Cell Quest; BD Biosciences).

4.6. Cell cycle analysis.

Firstly, A549 cells were grown in each well of six-well plates at the density of 5×10^4 cells/mL of the RPMI-1640 medium with 10% FBS to the final volume of 2 mL. The plates were also incubated at an atmosphere of 5% CO₂ and 95% air at 37.0 °C for overnight, and incubated in the presence or absence of complex **9** and cisplatin at the indicated concentrations for 24 h. Secondly, cells were harvested by centrifugation and fixed in ice-cold 70% ethanol at -20 °C for overnight. After the ethanol was removed the next day, the cells were resuspended in the ice-cold PBS and incubated with 100 µg/mL RNase A at 37 °C for 30 min, followed by incubated with the DNA staining solution propidium iodide (PI) in the dark at 4 °C for another 30 minutes detected by flow cytometry, and the results analysis was performed with the system software (Cell Quest; BD Biosciences).

4.7. Immunofluorescence assay.

A549 cells were grown in each well of six-well plates at the density of 5×10^4 cells/mL of the RPMI-1640 medium with 10% FBS to the final volume of 2 mL. The plates were also incubated at an atmosphere of 5% CO₂ and 95% air at 37.0 °C for overnight, and incubated in the presence or absence of complex **9** and cisplatin at the indicated concentrations for 24 h. After that, cells were fixed with 4% paraformaldehyde at 37 °C for 30 minutes, and then permeabilized with 0.5% Triton X-100/PBS for 15 minutes. After blocking for 30 minutes in 5% BSA/PBS, cells were washed with ice-cold PBS and treated with α -tubulin for 2 h, and then tubulin was immunostained with monoclonal antibody to α -tubulin followed by fluorescence antibody. Finally, cells were visualized by fluorescence microscope after the nuclei of cells were labeled with DAPI.

4.8. Cell migration assay.

A549 cells were seeded in 6-well plates and allowed to grow to $\geq 95\%$ confluent, and then wounds were created perpendicular to the lines by 20 µL tips, and unattached cells were removed by washing with thrice in PBS. Then the calcium AM (1 mM stock solution in DMSO with 1:1500 dilution in PBS) was used to stain cells. After that, cells incubated in the presence or absence of complex **9** and cisplatin at the indicated concentrations for 24 h. After 24 h incubation, the cells were washed with ice-cold PBS, and then photographed to mark the final scratched tracks. The migration rates analyzed by Equation 1: Migration rate (%) = $(d_1 - d_2)/d_1$. The d_1 and d_2 represented the width of wound at 0 and 24 h, respectively.

4.9. Mitochondrial membrane potential (MMP) assay.

A549 cells were grown in each well of six-well plates at the density of 5×10^4 cells/mL of the RPMI-1640 medium with 10% FBS to the final volume of 2 mL. The plates were also incubated at an atmosphere of 5% CO₂ and 95% air at 37.0 °C for overnight, and incubated in the presence or absence of complex **9** and cisplatin at the indicated concentrations for 24 h. After 24 h incubation, cells were then stained with 2 μM 5,5',6,6'-Tetrachloro-1,1',3,3'-tetraethyl-imidacarbocyanine (JC-1) in the dark at 4 °C for another 30 minutes. After that, cells were harvested at 2000 rpm and washed ice-cold PBS analyzed by flow cytometry.

4.10. Reactive oxygen species (ROS) assay.

A549 cells were grown in each well of six-well plates at the density of 5×10^4 cells/mL of the RPMI-1640 medium with 10% FBS to the final volume of 2 mL. The plates were also incubated at an atmosphere of 5% CO₂ and 95% air at 37.0 °C for overnight, and incubated in the presence or absence of complex **9** and cisplatin at the indicated concentrations for 24 h. After 24 h incubation, cells were then incubated with DCFH-DA in the dark at 4 °C for another 30 minutes. After that, cells were harvested at 2000 rpm and washed ice-cold PBS analyzed by flow cytometry.

4.11. Western blot assay.

Western blot analysis was performed as described previously [43, 44]. A549 cells were grown in each well of six-well plates at the density of 5×10^4 cells/mL of the RPMI-1640 medium with 10% FBS to the final volume of 2 mL. The plates were also incubated at an atmosphere of 5% CO₂ and 95% air at 37.0 °C for overnight, and incubated in the presence or absence of complex **9** and cisplatin at the indicated concentrations for 24 h. After for 24 h treatment, cells were collected, centrifuged, and washed ice-cold PBS. The pellet was then re-suspended in lysis buffer containing 150 mM NaCl, 50 mM Tris (pH 7.4), 1% (w/v) sodium deoxycholate, 1% (v/v) Triton X-100, 0.1% (w/v) SDS, and 1 mM EDTA (Beyotime, China), and then the lysates were incubated at 37 °C for another 30 minutes, and centrifuged at 20000g at 4 °C for 10 minutes. The protein concentration in the supernatant was analyzed by the BCA protein assay reagents. Equal amounts of protein per line were separated on 12% SDS polyacrylamide gel electrophoresis and transferred to PVDF Hybond-P membrane (GE Healthcare). Membranes were incubated with 5% skim milk in Tris-buffered saline with Tween 20 (TBST) buffer for 1 h and then the membranes being gently rotated overnight at 4 °C. Membranes were then incubated with primary antibodies against Bcl-2, Bax, aspase-3 and caspase-9 or GAPDH for overnight at 4 °C. After that, washed thrice in TBST, and then the membranes were next

incubated with peroxidase labeled secondary antibodies for another 2 h. Finally, all membranes were washed with TBST four times for 20 minutes and then the protein blots were detected by chemiluminescence reagent (Thermo Fischer Scientifics Ltd.). The X-ray films were developed with developer and fixed with fixer solution.

4.12. Anti-tumor activity *in vivo*.

The *in vivo* cytotoxic activity of complex **9** was further investigated by human lung cells (A549) in BALB/c nude mice. Five-week-old female BALB/c nude mice were purchased from Shanghai Ling Chang biotechnology company (China); tumors were induced by a subcutaneous injection in their dorsal region of 1.0×10^7 cells in 100 mL of sterile PBS. Animals were randomly divided into five groups, and started on the second day. When the tumors reached a volume of 100-150 mm³ in all mice on day 18, the first group was injected with an equivalent volume of 5% dextrose via a tail vein as the vehicle control mice. No. 2 group was treated with cisplatin at the dose of 5 mg/kg once a week for three weeks. No. 3 group was treated with **1a** at the dose of 5 mg/kg every two days for three weeks. No. 4 and No. 5 groups were treated with complex **9** at doses of 5 mg/kg (equal mass dose of cisplatin) and 13 mg/kg (equal molar dose to cisplatin) once a week for three weeks, respectively. All tested compounds were dissolved in vehicle. Tumor volume and body weight were recorded every other day after drug treatment. We collected and weighed the tumors and calculated the inhibition rate of tumor growth (IRT) at the end of treatment. All mice were sacrificed after three weeks of treatment and the tumor volumes were measured with electronic digital calipers and determined by measuring length (A) and width (B) to calculate volume ($V = AB^2/2$).

Notes

The authors declare no competing financial interest.

Acknowledgments

We are grateful to the National Natural Science Foundation of China (Grant Nos. 21977021, 81760626 and 22007036) and the China Postdoctoral Science Foundation (2020M673553XB), and the Ministry of Education Innovation Team Fund (IRT_16R15, 2016GXNSFGA380005). In addition, we would like to thank the Natural Science Foundation of Guangxi Province (AB17292075) and Guangxi Funds for Distinguished Experts. Finally, we are also very grateful to the Open Project Program of the National & Local Joint Engineering Research Center for Mineral Salt Deep Utilization (SF201904), and the Major projects of natural science research in Colleges

and universities of Jiangsu Province (18KJA530002), and the Jiangsu Industry-University-Research Cooperative Program (BY2019169).

References

- [1] C.J. Tsai, R. Nussinov, The molecular basis of targeting protein kinases in cancer therapeutics, *Semin. Cancer Biol.* 23 (2013) 235-242.
- [2] F. Pellegrini, D.R. Budman, Review: tubulin function, action of antitubulin drugs, and new drug development, *Cancer Invest.* 23 (2005) 264-273.
- [3] P. Suman, T. R. Murthy, K. Rajkumar, D. Srikanth, C. Dayakar, C. Kishor, A. Addlagatta, S. V. Kalivendi, B.C. Raju, Synthesis and structure-activity relationships of pyridinyl-1H-1,2,3-triazolyldihydroisoxazoles as potent inhibitors of tubulin polymerization, *Eur. J. Med. Chem.* 90 (2015) 603-619.
- [4] V. Chaudhary, J. B. Venghateri, H. P. Dhaked, A. S. Bhoyar, S. K. Guchhait, D. Panda, Novel combretastatin-2-aminoimidazole analogues as potent tubulin assembly Inhibitors: exploration of unique pharmacophoric impact of bridging skeleton and aryl moiety, *J. Med. Chem.* 59 (2016) 3439-3451.
- [5] C. Dumontet, M.A. Jordan, Microtubule-binding agents: a dynamic field of cancer therapeutics, *Nat. Rev. Drug Discovery.* 9 (2010) 790-803.
- [6] M.A. Jordan, L. Wilson, Microtubules as a target for anticancer drugs, *Nat. Rev. Cancer.* 4 (2004) 253-265.
- [7] B. An, B. Wang, J. Hu, S. Xu, L. Huang, X. Li, and A.S.C. Chan, Synthesis and biological evaluation of selenium-containing 4-anilinoquinazoline derivatives as novel antimitotic agents, *J. Med. Chem.* 61 (2018) 2571-2588.
- [8] A. Dowlati, K. Robertson, M. Cooney, W.P. Petros, M. Stratford, J. Jesberger, N. Rafie, B. Overmoyer, V. Makkar, B. Stambler, A. Taylor, J. Waas, J.S. Lewin, K.R. McCrae, S.C. Remick, A phase I pharmacokinetic and translational study of the novel vascular targeting agent combretastatin A-4 phosphate on a single-dose intravenous schedule in patients with advanced cancer, *Cancer Res.* 62 (2002) 3408-3416.
- [9] G.J. Rustin, S.M. Galbraith, H. Anderson, M. Stratford, L.K. Folkes, L. Sena, L. Gumbrell, P.M. Price, Phase I clinical trial of weekly CA-4 phosphate: clinical and pharmacokinetic results, *J. Clin. Oncol.* 21 (2003) 2815-2822.

- [10] R. Schobert, B. Biersack, A. Dietrich, S. Knauer, M. Zoldakova, A. Fruehauf, T. Mueller, Pt(II) complexes of a combretastatin A-4 analogous chalcone: effects of conjugation on cytotoxicity, tumor specificity, and long-term tumor growth suppression, *J. Med. Chem.* 52 (2009) 241-246.
- [11] M.O. Steinmetz, A.E. Prota, Microtubule-targeting agents: strategies to hijack the cytoskeleton, *Trends Cell Biol.* 28 (2018) 776–792.
- [12] S. Hua, F. Chen, S. Gou, Microtubule inhibitors containing immunostimulatory agents promote cancer immunochemotherapy by inhibiting tubulin polymerization and tryptophan-2,3-dioxygenase, *Eur. J. Med. Chem.* 187 (2020) 111949.
- [13] N.S. Vasudev, A.R. Reynolds, Anti-angiogenic therapy for cancer: current progress, unresolved questions and future directions, *Angiogenesis* 17 (2014) 471-494.
- [14] G. Wang, C. Li, L. He, K. Lei, F. Wang, Y. Pu, Z. Yang, D. Cao, L. Ma, J. Chen, Y. Sang, X. Liang, M. Xiang, A. Peng, Y. Wei, L. Chen, Design, synthesis and biological evaluation of a series of pyrano chalcone derivatives containing indole moiety as novel anti-tubulin agents, *Bioorg. Med. Chem.* 22 (2014) 2060-2079.
- [15] D. Wang, S.J. Lippard, Cellular processing of platinum anticancer drugs, *Nat. Rev. Drug Discov.* 4 (2005) 307-320.
- [16] K.B. Huang, F.Y. Wang, X.M. Tang, H.W. Feng, Z.F. Chen, Y.C. Liu, Y.N. Liu, and H. Liang, Organometallic gold(III) complexes similar to tetrahydroisoquinoline induce ER-stress-mediated apoptosis and pro-death autophagy in A549 cancer cells, *J. Med. Chem.* 61 (2018) 3478-3490.
- [17] E.R. Jamieson, S. Lippard, Structure, recognition, and processing of cisplatin DNA adducts, *J. Chem. Rev.* 99 (1999) 2467-2498.
- [18] X. Qin, L. Fang, F. Chen, S. Gou, Conjugation of platinum(IV) complexes with chlorambucil to overcome cisplatin resistance via a “joint action” mode toward DNA, *Eur. J. Med. Chem.* 137 (2017) 167-175.
- [19] A.S. Abu-Surrah, M. Kettunen, Platinum group antitumor chemistry: design and development of new anticancer drugs complementary to cisplatin, *Curr. Med. Chem.* 13 (2006) 1337-1357.
- [20] Z. Liu, M. Wang, H. Wang, L. Fang, and S. Gou, Platinum-based modification of styrylbenzylsulfones as multifunctional antitumor agents: Targeting the RAS/RAF pathway, enhancing antitumor activity, and overcoming multidrug resistance, *J. Med. Chem.* 63 (2020)

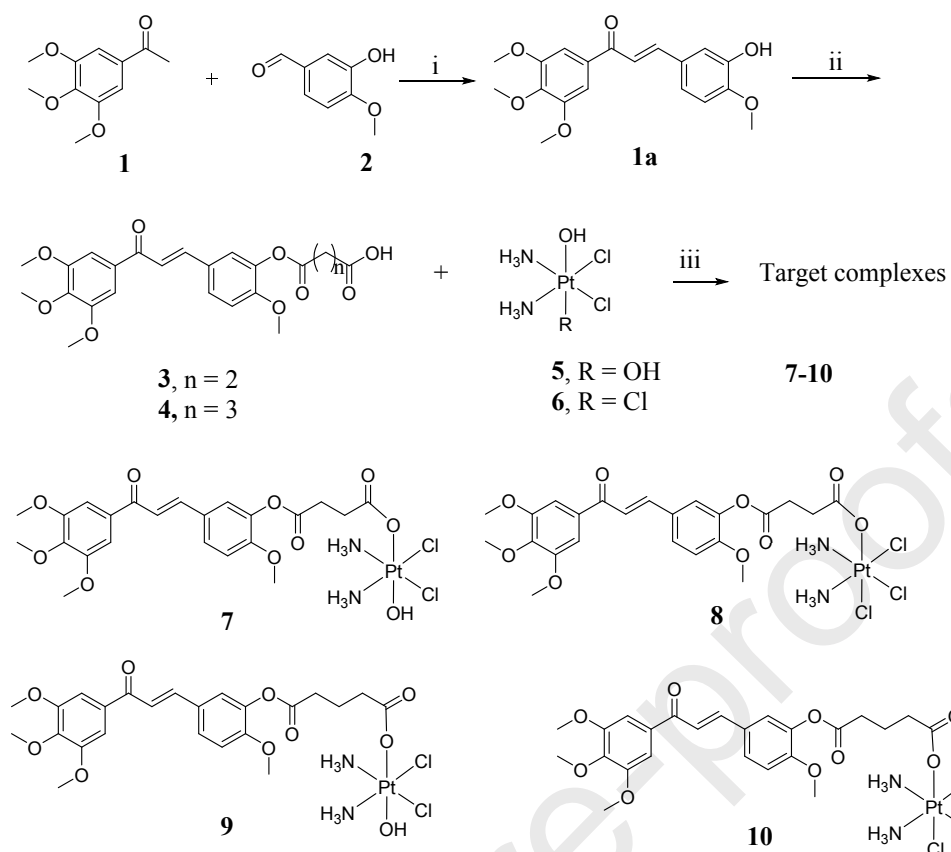
186-204.

- [21] W. Zhang, Z. Zhang and C.H. Tung, Beyond chemotherapeutics: cisplatin as a temporary buckle to fabricate drug-loaded nanogels, *Chem. Comm.* 53 (2017) 779-782.
- [22] C.A. Rabik, M.E. Dolan, Molecular mechanisms of resistance and toxicity associated with platinating agents, *Cancer Treat. Rev.* 33 (2007) 9-23.
- [23] X.P. Han, S. Jin, Y.J. Wang, Z.G. He, Recent advances in platinum(IV) complex based delivery systems to improve platinum(II) anticancer therapy, *Med. Res. Rev.* 35 (2015) 1268-1299.
- [24] T.C. Johnstone, K. Suntharalingam, S.J. Lippard, The next generation of platinum drugs: targeted Pt(II) agents, nanoparticle delivery, and Pt(IV) prodrugs, *Chem. Rev.* 116 (2016) 3436-3486.
- [25] J. Lorenzo, A. Delgado, Á.M. Montaña, J.M. Mesas, M.T. Alegre, M.C. Rodríguez, F.X. Avilés, Synthesis, biological evaluation and SAR studies of novel bicyclic antitumor platinum(IV) complexes, *Eur. J. Med. Chem.* 83 (2014) 374-388.
- [26] L. Fang, X. Qin, J. Zhao, and S. Gou, Construction of dual stimuli-responsive platinum(IV) hybrids with NQO1 targeting ability and overcoming cisplatin resistance, *Inorg. Chem.* 58 (2019) 2191-2200.
- [27] R.K. Pathak, S. Marrache, J.H. Choi, T.B. Berding, S. Dhar, The Pro-drug platin-A: simultaneous release of cisplatin and aspirin, *Angew. Chem. Int. Ed.* 53 (2014) 1963-1967.
- [28] X. Xue, S. You, Q. Zhang, Y. Wu, G.Z. Zou, P. C. Wang, Y.L. Zhao, Y. Xu, L. Jia, X. Zhang, and X.J. Liang, Mitaplatin increases sensitivity of tumor cells to cisplatin by inducing mitochondrial dysfunction, *Mol. Pharmaceutics.* 9 (2012) 634-644.
- [29] Z.G. Wang, Z.F. Xu, G.Y. Zhu, A platinum(IV) anticancer prodrug targeting nucleotide excision repair to overcome cisplatin resistance, *Angew. Chem., Int. Ed.* 55 (2016) 15564-15568.
- [30] (a) F. Chen, X. Huang, M. Wu, S. Gou, W.W. Hu, A CK2-targeted Pt(IV) prodrug to disrupt DNA damage response, *Canc. Lett.* 385 (2017) 168-178. (b) X. Huang, M. Wang, C. Wang, W. Hu, Q. You, Y. Yang, C. Yu, Z. Liao, S. Gou, H. Wang, Dual-targeting antitumor conjugates derived from platinum(IV) prodrugs and microtubule inhibitor CA-4 significantly exhibited potent ability to overcome cisplatin resistance, *Bioorg. Chem.* 92 (2019) 103236.
- [31] (a) M. Ravera, E. Gabano, G. Pelosi, F. Fregonese, S. Tinello, D. Osella, A new entry to asymmetric platinum(IV) complexes via oxidative chlorination, *Inorg. Chem.* 53 (2014) 9326-

9335. (b) X.Q. Song, Z.Y. Ma, Y.G. Wu, M.L. Dai, D.B. Wang, J.Y. Xu, Y. Liu, New NSAID-Pt(IV) prodrugs to suppress metastasis and invasion of tumor cells and enhance anti-tumor effect in vitro and in vivo, *Eur. J. Med. Chem.* 167 (2019) 377-387.
- [32] Y. Chen, J. Huang, S. Zhang, and Z. Gu, Superamphiphile based cross-linked small-molecule micelles for pH-triggered release of anticancer drugs, *Chem. Mater.* 29 (2017) 3083-3091.
- [33] J.J. Chen, J.X. Ding, W.G. Xu, T.M. Sun, H.H. Xiao, X.L. Zhuang, X.S. Chen, Receptor and microenvironment dual-recognizable nanogel for targeted chemotherapy of highly metastatic malignancy, *Nano Lett.* 17 (2017) 4526-4533.
- [34] S. Wen, D. Zhu, and P. Huang, Targeting cancer cell mitochondria as a therapeutic approach, *Future Med. Chem.* 5 (2013) 53-67.
- [35] F. Dai, Q. Li, Y. Wang, C. Ge, C. Feng, S. Xie, H. He, X. Xu, C. Wang, Design, synthesis, and biological evaluation of mitochondria targeted flavone-naphthalimide-polyamine conjugates with antimetastatic activity, *J. Med. Chem.* 60 (2017) 2071-2083.
- [36] C.Y. Liu, C.F. Lee, Y.H. Wei, Role of reactive oxygen species-elicited apoptosis in the pathophysiology of mitochondrial and neurodegenerative diseases associated with mitochondrial DNA mutations, *J. Formosan Med. Assoc.* 108 (2009) 599-611.
- [37] Z. Liu, M. Wang, H. Wang, L. Fang, S. Gou, Targeting RAS-RAF pathway significantly improves antitumor activity of Rigosertib-derived platinum(IV) complexes and overcomes cisplatin resistance, *Eur. J. Med. Chem.* 194 (2020) 112269.
- [38] N. Muhammad, C.P. Tan, U. Nawaz, J. Wang, F.X. Wang, S. Nasreen, L.N. Ji, Z.W. Mao, Multi-action platinum(IV) prodrug containing thymidylate synthase inhibitor and metabolic modifier against triple-negative breast cancer, *Inorg. Chem.* 59 (2020) 12632-12642.
- [39] H.U. Simon, A. Haj-Yehia, F. Levi-Schaffer, Role of reactive oxygen species (ROS) in apoptosis induction, *Apoptosis* 5 (2000) 415-418.
- [40] J.S. Clerkin, R. Naughton, C. Quiney, T.G. Cotter, Mechanisms of ROS modulated cell survival during carcinogenesis, *Canc. Lett.* 266 (2008) 30-36.
- [41] T. Moldoveanu, A.V. Follis, R.W. Kriwacki, D.R. Green, Many players in Bcl-2 family affairs, *Trends Biochem. Sci.* 39 (2014) 101-111.
- [42] P. Monian, X. Jiang, Clearing the final hurdles to mitochondrial apoptosis: regulation post cytochrome c release, *Exp. Oncol.* 34 (2012) 185-191.

- [43] S.H. Huang, L.W. Wu, A.C. Huang, C.C. Yu, J.C. Lien, Y.P. Huang, J.S. Yang, J.H. Yang, Y.P. Hsiao, W.G. Wood, C.S. Yu, J.G. Chung, Benzyl isothiocyanate (BITC) induces G2/M phase arrest and apoptosis in human melanoma A375.S2 cells through reactive oxygen species (ROS) and both mitochondria dependent and death receptor-mediated multiple signaling pathways, *J. Agric. Food Chem.* 60 (2012) 665-675.
- [44] J. Yan, J. Chen, S. Zhang, J.H. Hu, L. Huang, and X.S. Li, Synthesis, evaluation, and mechanism study of novel indole-chalcone derivatives exerting effective antitumor activity through microtubule destabilization *in vitro* and *in vivo*, *J. Med. Chem.* 59 (2016) 5264-5283.

Schemes:



Scheme 1. Synthetic pathway to target compounds **7-10**. Reagents and conditions: (i) KOH (50% w/v aqueous solution), CH₃OH, 0 °C, overnight; (ii) Succinic anhydride or glutaric anhydride, K₂CO₃, DMF, 50 °C.; (iii) TBTU, Et₃N, DMF, 30 °C.

Table 1. Cytotoxic effects of complexes **7-10** on human cancer and normal cell lines.

Compds.	IC ₅₀ (μM) ^a					
	HeLa	MGC-803	HepG-2	NCI-H460	HL-7702	SI ^b
3	0.78±0.14	1.35±0.19	0.81±0.23	0.97±0.13	9.24±1.53	11.4
4	0.52±0.12	1.16±0.18	0.69±1.46	0.78±0.16	10.25±1.34	14.8
7	0.41±0.09	0.30±0.07	0.33±0.08	0.45±0.12	11.85±1.37	35.9
8	0.50±0.12	0.45±0.09	0.41±0.05	0.61±0.10	12.03±1.41	29.3
9	0.32±0.03	0.26±0.06	0.29±0.04	0.37±0.09	12.35±1.83	42.6
10	0.43±0.09	0.39±0.10	0.35±0.07	0.55±0.13	13.08±1.56	37.4
1a	0.65±0.05	0.55±0.14	0.42±0.09	0.72±0.08	3.07±0.72	7.3
Cisplatin	9.41±1.09	6.56±1.18	8.01±1.24	7.85±1.32	10.36±1.43	1.3

^a *In vitro* cytotoxicity was determined by MTT assay upon incubation of the live cells with the compounds for 72 h. ^b Selectivity Index = IC₅₀(HL-7702)/IC₅₀(HepG-2). Mean values based on three independent experiments.

Table 2. Anti-proliferative activities of optimal complex **9** on the cisplatin-resistant cells A549 and the doxorubicin-resistant cells MCF-7.

Compds.	IC ₅₀ (μM) ^b					
	A549	A549/CDDP	RF ^c	MCF-7	MCF-7/DOX	RF ^c
9	0.19±0.04	0.23±0.06	1.2	0.38±0.09	0.42±0.11	1.1
1a	0.43±0.08	0.72±0.14	1.7	0.95±0.08	1.52±0.54	1.6
4	0.65±0.13	0.83±0.11	1.3	1.76±0.27	2.33±0.39	1.3
4+CDDP	0.54±0.14	1.09±0.17	2.0	1.15±0.16	1.77±0.22	1.5
DOX ^a	2.15±0.26	5.24±0.53	2.4	3.03±0.08	42.71±2.01	14.1
CDDP	6.43±1.15	35.06±2.31	5.5	6.38±1.02	9.05±1.33	1.4

^a Doxorubicin; ^b *In vitro* cytotoxicity was determined by MTT assay upon incubation of the live cells with the compounds for 72 h; ^c Resistant factor = (IC₅₀ human resistance cells)/(IC₅₀ human cancer sensitive cells).

Table 3. Cellular uptake of complex **9** in A549 cells.

Compounds	Pt content (ng/10 ⁶ cells) ^b
	A549
9 (5 μ M)	126 \pm 15
9 (10 μ M)	263 \pm 32
Cisplatin (5 μ M)	72 \pm 9
Cisplatin (10 μ M)	117 \pm 13

The experiments were performed three times, and the results of the representative experiments are shown.

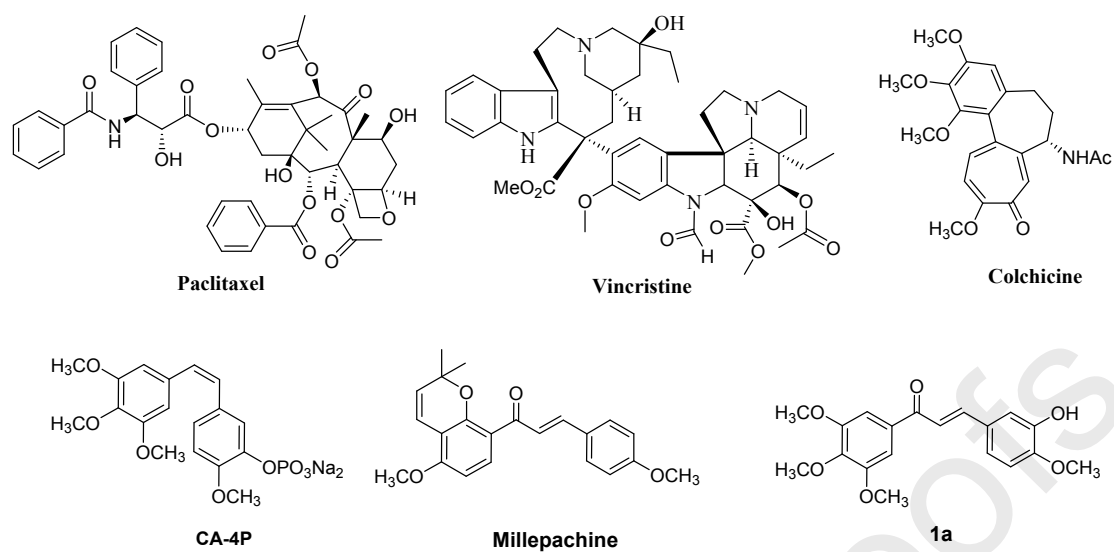


Fig.1. Structures of natural products and chalcone analogues as potent inhibitors of tubulin polymerization.

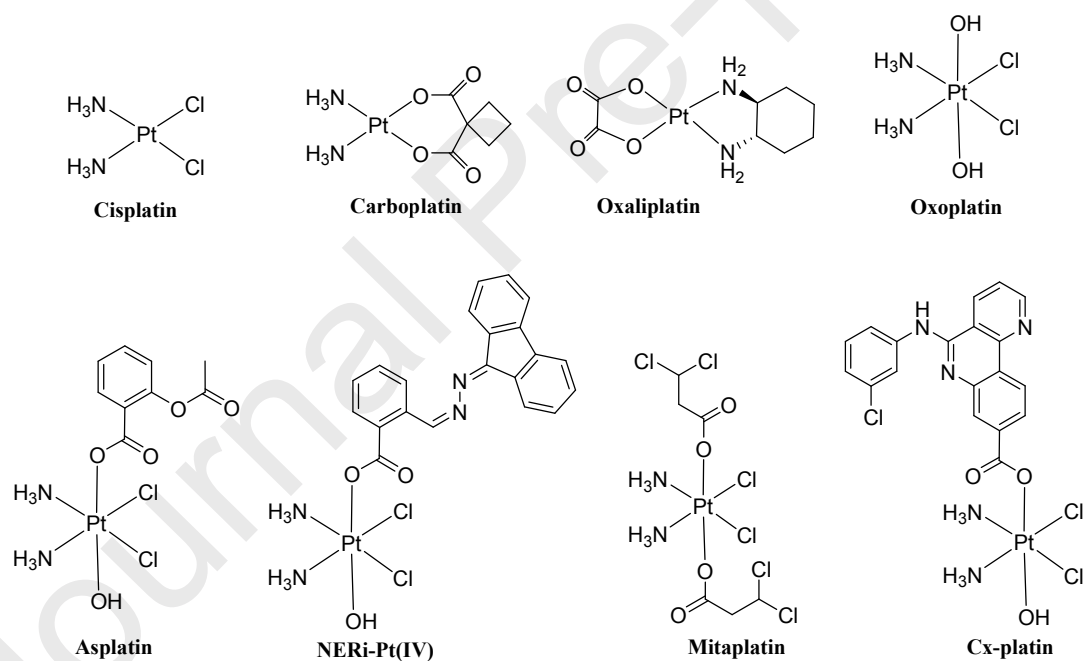


Fig. 2. FDA approved platinum(II) anticancer agents and chemical structures of some platinum(IV) complexes as prodrugs.

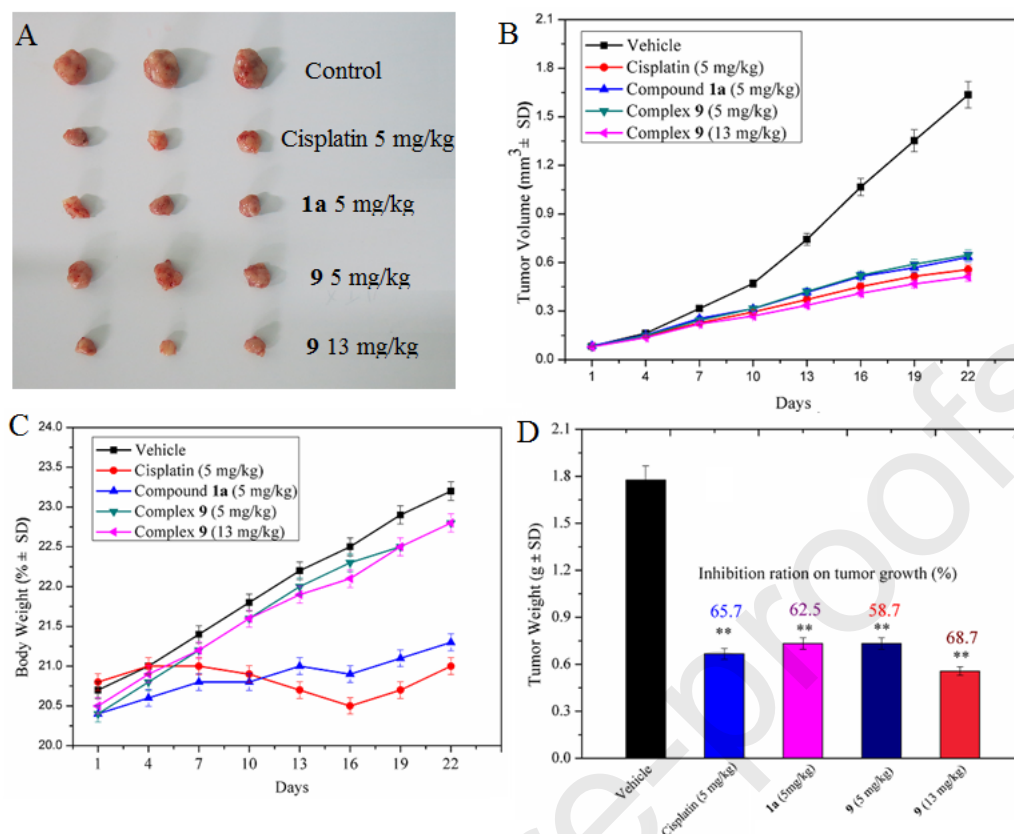


Fig. 3. *In vivo* anticancer effect of complex 9 on A549 xenograft models. Fifteen mice were randomly divided into five groups, No. 1 group was injected with equal dose of saline was used as control group, No. 2 group was treated with cisplatin at the dose of 5 mg/kg once a week for three weeks, No. 3 group was treated with **1a** at the dose of 5 mg/kg every two days for three weeks, No. 4 and No. 5 groups were treated with complex 9 at doses of 5 mg/kg and 13 mg/kg once a week for three weeks, respectively. (A) Tumor images obtained from mice of various groups. (B) The tumor volume of the mice in each group during the observation period. (C) The body weight of the mice from each group at the end of the observation period. (D) The weight of the excised tumors of each group. The data were presented as the mean \pm SEM. IR=Inhibitory rate. * $P < 0.05$

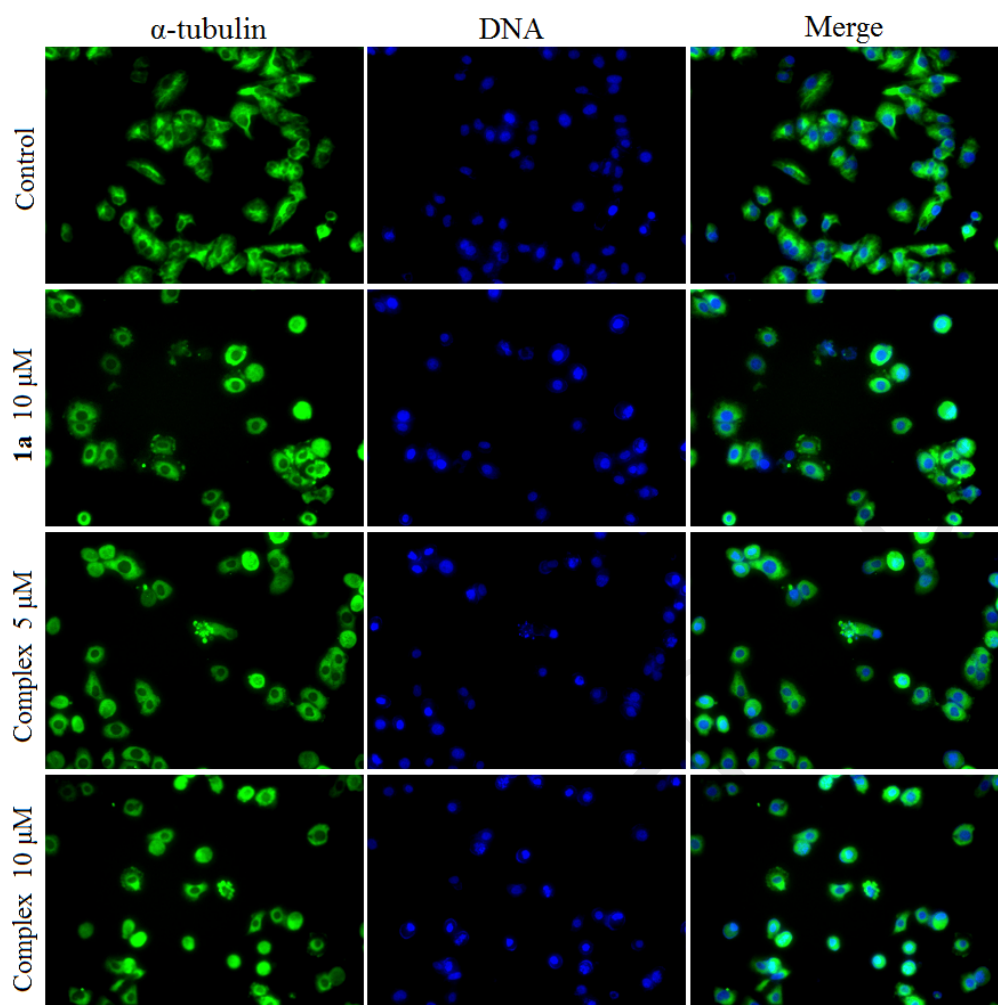


Fig. 4. Effects of complex **9** on the microtubule network of cells. After 24 h co-treatment with complex **9** (5 and 10 μ M), A549 cells were fixed in paraformaldehyde (4 %), stained with α -tubulin and DAPI, and the images were recorded via laser confocal microscope. Microtubules and unassembled tubulin are shown in green, and DNA stained in blue. The results represent one of three independent experiments.

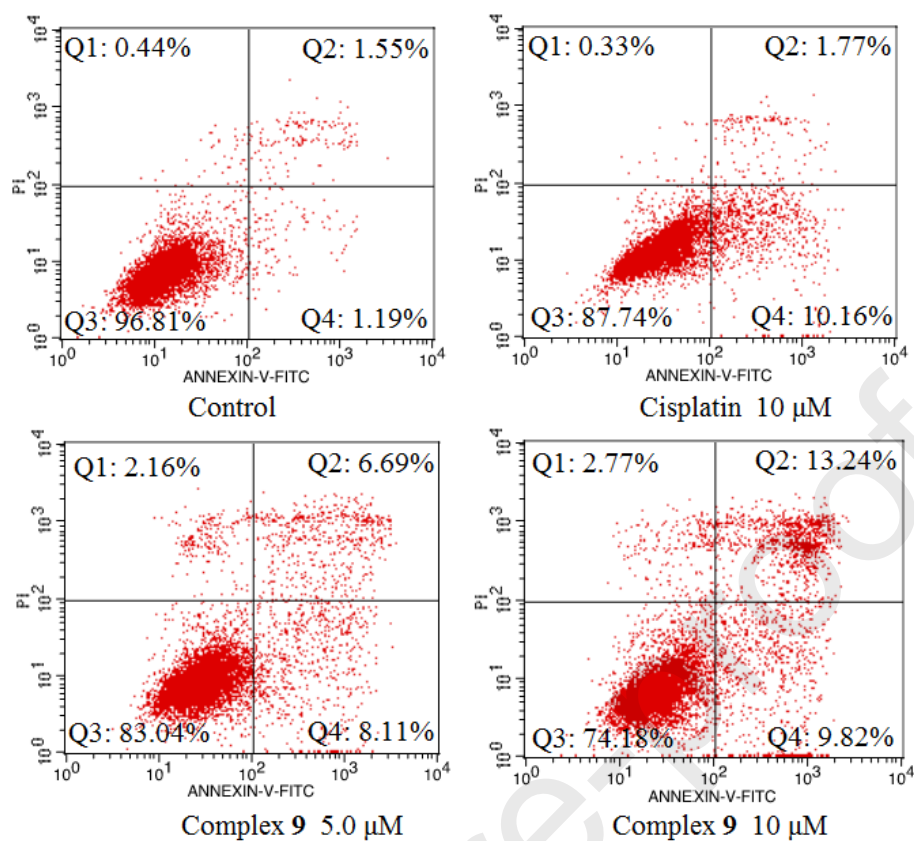


Fig. 5. Apoptosis in A549 cells induced by complex 9. Upon treatment with complex 9 (5, 10 μ M) or cisplatin (10 μ M) for 24 h. The cells were harvested, labeled with annexin-V-FITC and PI, and analyzed by flow cytometry. Data are expressed as the mean \pm SEM for three independent experiments.

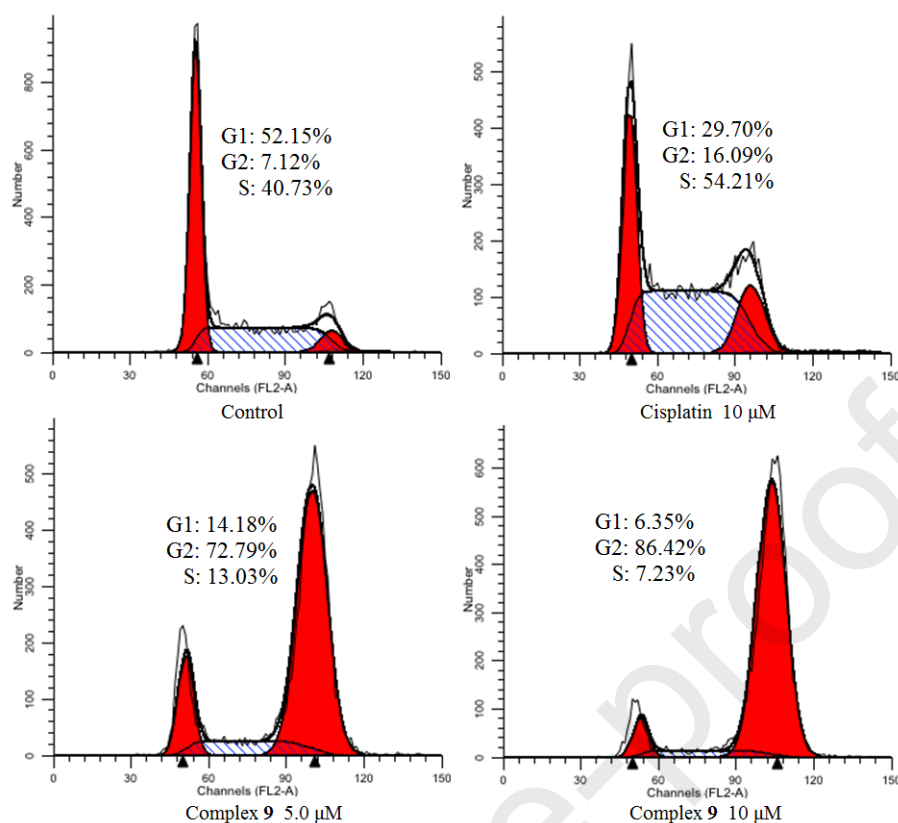


Fig. 6. Effects of compound **9** on cell cycle progression. A549 cells treated with compound **9** (5 and 10 μ M) and cisplatin (10 μ M) for 24 h, were harvested for flow cytometry analysis. The results were shown as one of three independent experiments.

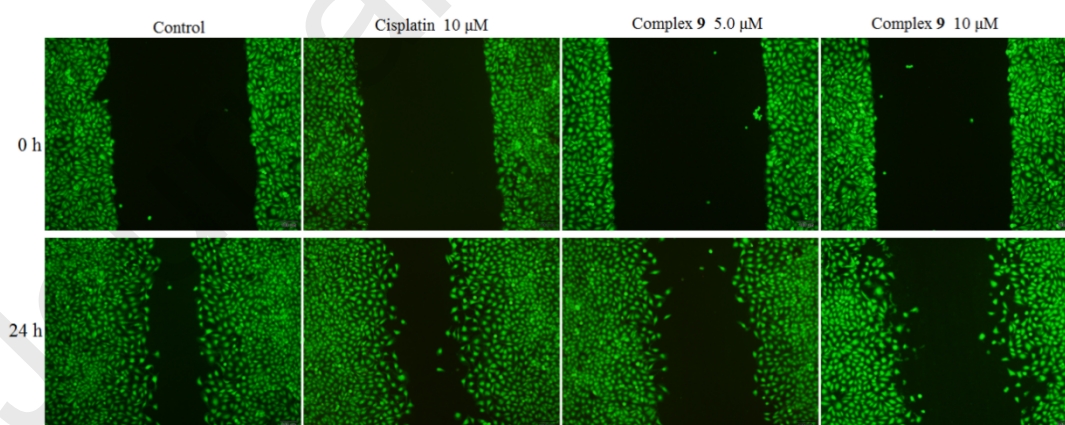


Fig. 7. Migration inhibitory effects of complex **9** on A549 cells. Cells were treated with compound **9** (5, 10 μ M) or cisplatin (10 μ M) for 24 h, respectively, and were stained with calcein AM. Typical images were taken at 0 and 24 h.

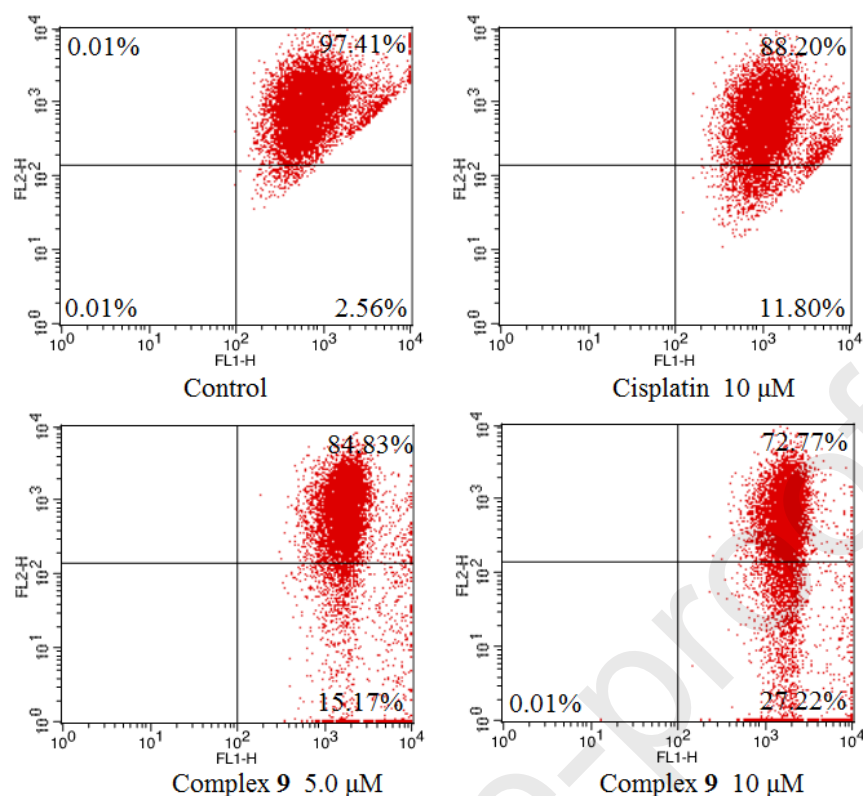


Fig. 8. MMP collapse induced by complex 9 in A549 cells. A549 cells were treated with complex 9 and cisplatin at the indicated concentrations for 24 h followed by incubation with the fluorescence probe JC-1 for 30 min. Then, the cells were harvested for flow cytometry analysis. The results were presented as one of three independent experiments.

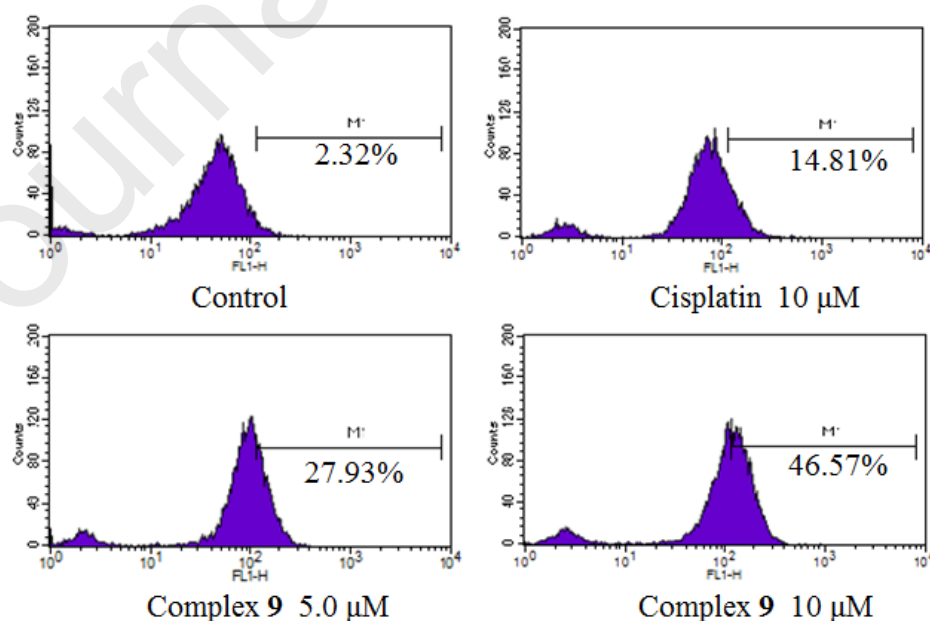


Fig. 9. Complex 9 induced intracellular ROS accumulation. After 24 h co-incubation with complex

9 (5 and 10 μM) or cisplatin (10 μM), A549 cells were harvested, stained with DCFH-DA and analyzed with flow cytometry. The results were shown as one of three independent experiments.

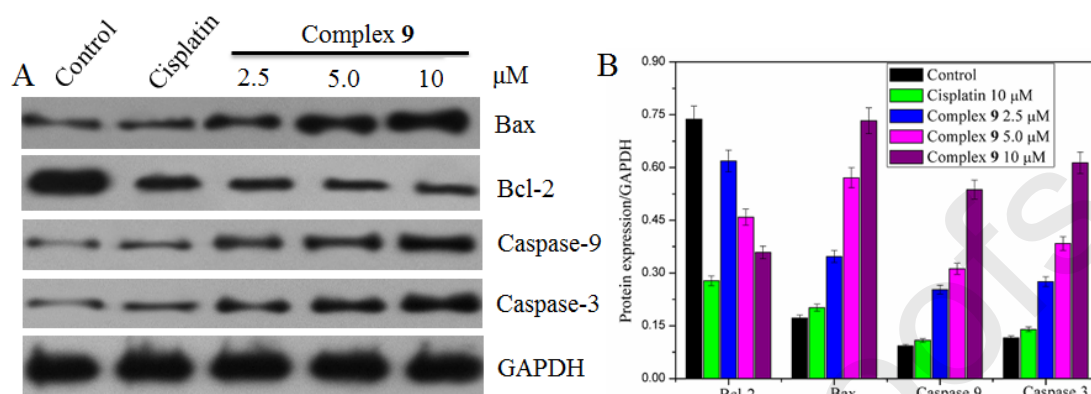
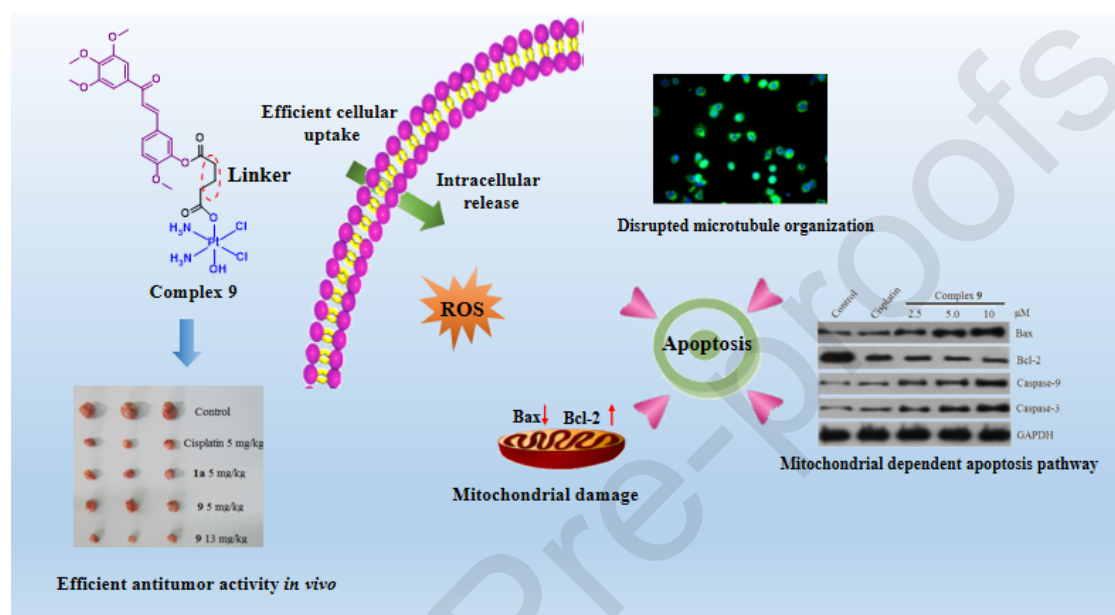


Fig. 10. The effects of complex **9** on the apoptosis-related protein. A549 cells of 24 h incubation with complex **9** (2.5, 5 and 10 μM) or cisplatin (10 μM) were collected for western blotting assays. (A) Representative western blots in complex **9** treated A549 cells. GAPDH was used as internal control. (B) Percentage expression levels of Bcl-2, Bax, caspase-9 and caspase-3. The percentage values are normalized with GAPDH.

Graphical abstract

Platinum(IV) complexes conjugated with chalcone analogs as dual targeting anticancer agents: *in vitro* and *in vivo* studies

Xiaochao Huang^{a, b 1}, Zhikun Liu^{c 1}, Meng Wang^{a *}, Xiulian Yin^a, Yanming Wang^a, Lumei Dai^{d *} and Hengshan Wang^{b *}



Highlights

- **9** exhibited nanomole level in inhibiting anticancer proliferation but share better selectivity of HL-7702 cells.
- **9** efficiently overcome multidrug resistance against A549 and A549/CDDP cells.
- **9** remarkably disrupted the microtubule biological function.
- **9** might induce A549 cells apoptosis through mitochondrion pathway.
- **9** exerted efficient antitumor activities *in vivo* with better drug safety properties.

Declaration of interests

☒ The authors declare that they have no known competing financial interests or personal relationships that could have appeared to influence the work reported in this paper.

☐ The authors declare the following financial interests/personal relationships which may be considered as potential competing interests: